Supplemental Material

Visual discrimination training. Rats were trained to respond on a touchscreen [52] for sweetened condensed milk (30%; 0.1 ml/reinf) with behavioral programs coded and run using E-Prime software (Psychology Software Tools, Pittsburgh, PA). During these initial training sessions, rats were required to make 100 responses on a response box which was initially stationary and later appeared in different locations to ensure spatial discrimination.

Following acquisition of responding, rats were trained in a visual discrimination task. Using a 5-stage stimulus-fading procedure, rats were trained to discriminate between detailed photographic stimuli (green leaf/violet flower) during daily, 100-trial sessions on a FR1 schedule of reinforcement. The goal of the fading procedure was to allow rats to initially acquire discrimination behavior using large stimuli, and then to reduce the size of the stimuli to a size permitting two images to "flank" the target image. During discrimination training, a 5 KHz and a 15 KHz tone (counterbalanced) signaled correct and incorrect responses, and incorrect responses resulted in a 20-sec timeout period. During the first two training stages, a correction procedure was used in which an incorrect response resulted in a repeated trial until a correct response was made [53]. Once initial discrimination was established, rats progressed through the remaining stages of the fading procedure with no correction rule in place. In each training stage, discrimination was deemed successful when the criterion of 70% response accuracy during the session was recorded on two consecutive days.

Cross-species electroencephalographic recording and data reduction. In humans, continuous electroencephalographic (EEG) activity was recorded from a customized 96-

channel actiCAP system using an actiCHamp amplifier (Brain Products GmbH, Gilching, Germany). Impedances were kept below 25kΩ. The ground channel was embedded in the cap and was located anterior and to the right of channel 10, which roughly corresponds to electrode Fz. During data acquisition, channel 1 (Cz) served as the online reference channel. All signals were digitized at 500Hz using BrainVision Recorder software (Brain Products).

Offline analyses were performed using BrainVision Analyzer 2.0 (Brain Products). Gross muscle artifacts and EEG data during the breaks in-between blocks were first manually removed by visual inspection. The data were band-pass filtered with cutoffs of 0.1 and 30Hz, 24dB/oct rolloff. Blinks, horizontal eye movements, and electrocardiogram were removed using independent component analysis (ICA), and corrupted channels were interpolated using spline interpolation [54]. Scalp electrode recordings were re-referenced to the average activity of all electrodes.

In rats, continuous EEG and LFP data were recorded during each Flanker task test session using the RHD-2000 recording system and supported data acquisition software (Intan Technologies). Signals were digitized locally via a head-mounted RHD 16-channel amplifier board (Intan Technologies). Data were continuously sampled at 1KHz with a bandwidth range of 0.1-300Hz for the duration of the behavioral session. Following the session, offline analyses were performed using BrainVision Analyzer 2.0 (Brain Products). Data were down-sampled to 500Hz and referenced to the left cerebellar screw electrode.

Cross-species data analysis. For the behavioral data, the two species were directly compared in their Flanker interference (accuracy) effects using a univariate analysis with *Species* and *Sex* as

between subject factors. For the EEG analyses, data were first normalized to account for cross-species differences in signal strength/electrode type. For dependent variables that can only be positive (e.g., spectral power), data were normalized as percent change [(incongruent-congruent)/(incongruent + congruent)]. For dependent variables that could be positive or negative (e.g., ERN), such normalization was not possible because it could have led to denominators close to zero, and, as a result, artificially inflated normalized data. Accordingly, to compare ERP task effects, we used a data-driven approach based on the assumption that the distributions of amplitudes in the rat local field potential is a scaled version of the human ERP. Under this assumption, both the ratios between the means and between standard deviations of amplitudes in rats and humans can be estimates of the scaling factor. We choose the ratio between standard deviations since 1) it is by definition always positive and 2) it is numerically more stable than the ratio between means. This scaling factor (ratio of cross-species standard deviations) was calculated in a trial type-specific way to allow for the possibility of biologically-relevant differences in variance of neurophysiological activity by trial type. Once data were transformed, differences between incorrect and correct responses were compared across species. For these analyses, data for the 16mg/kg dose in rats were excluded to match the number of conditions for each species. For figures depicting electrophysiological results, only channels in which significant differences were detected are shown.

To provide broader context regarding the statistical power of our modafinil analyses, we performed a post hoc Bayes Factor analysis on all main effects evaluated in both species. Each main effect was compared to the null hypothesis and the resultant BF_{10} values are reported in the Results section. In this case, BF_{10} values are a ratio of the likelihood of a main effect to the null hypothesis.

A BF_{10} value of 1 indicates there is no evidence for either hypothesis, while BF_{10} values below 1 indicate that the null hypothesis is more likely than the main effect. BF_{10} values above 1 indicate the main effect is more likely than the null hypothesis; values from 1-3 indicate anecdotal evidence, values from 3-10 indicate moderate evidence, values from 10-30 indicate strong evidence, values from 30-100 indicate very strong evidence, and values >100 indicate extreme evidence [55].

Due to a lack of apparent differentiation between conditions in the rat stimulus-locked ERPs, data from each time frame (at 1000Hz, this corresponds to 1000 data points per second) were entered into a TANOVA (topographic analysis of variance) using standardized low-resolution electromagnetic tomography (sLORETA; [37]). The congruency effect (incongruent minus congruent) was computed using paired-samples t-tests. A total of 5,000 randomizations were performed to compute a t distribution, critical thresholds and p-values that correct for the number of statistical comparisons.

Finally, to determine source localization of the human ERN and N200 we used sLORETA. Activity in the ±10ms (20ms total) time window around the grand average difference wave peaks for the ERN and N200 was statistically analyzed using two-tailed *t*-tests for dependent samples. The differences in localization between conditions (error minus correct, incongruent minus congruent) were computed by voxel-by-voxel *t*-tests for dependent measures after subject-wise normalization. A total of 5,000 randomizations were performed to compute critical thresholds and p-values that corrected for multiple testing.

REFERENCES

52. Kangas, B. D., & Bergman, J. Touchscreen technology in the study of cognition-related behavior. Behav Pharmacol. 2017;28:623-629.

53. Kangas BD, & Branch MN. Empirical validation of a procedure to correct position and stimulus biases in matching-to-sample. J Exp Anal Behav. 2008;90:103-112.

54. Perrin F, Pernier J, Bertnard O, Giard MH, & Echallier JF. Mapping of scalp potentials by surface spline interpolation. Electroencephalogr Clin Neurophysiol. 1987;66:75-81.

55. Lee MD, & Wagenmakers EJ. Bayesian cognitive modeling: A practical course. Cambridge University press; 2014.

Concordant neurophysiological signatures of cognitive control in humans and rats

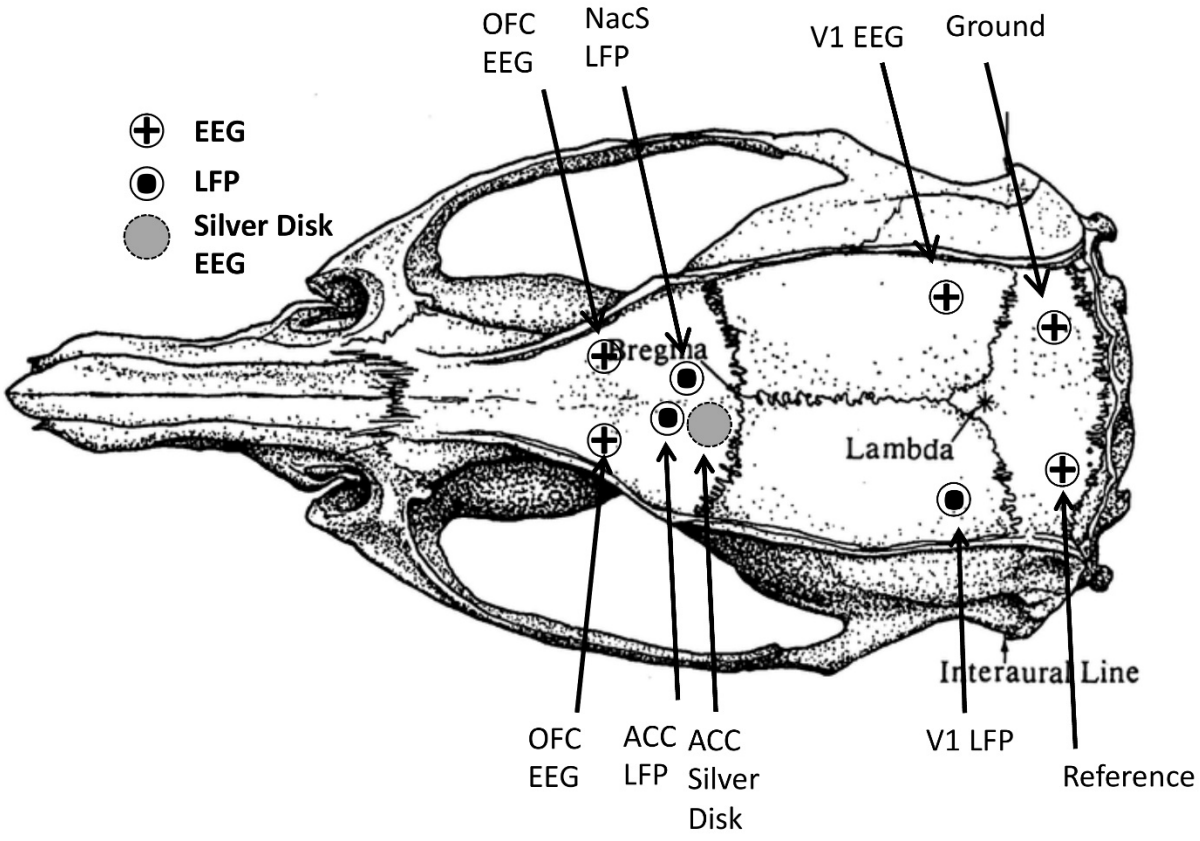

Supplemental Figure 1: Schematic of rat electrode placements. Skull screw electrode placements are indicated with "+"s, local field potential wires are indicated with closed black circles, and the silver disk electrode is indicated with a gray circle.

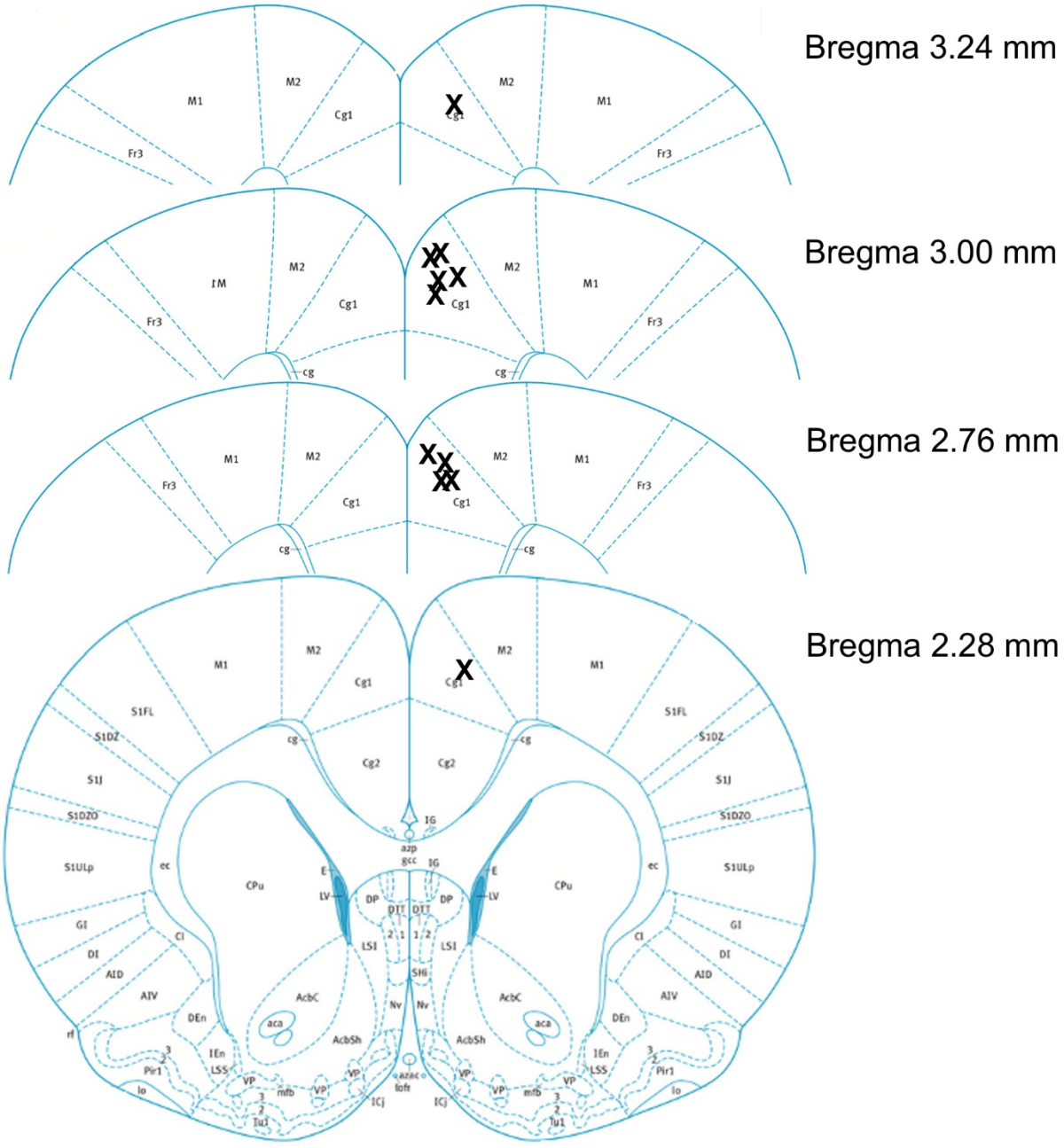

Supplemental Figure 2: Histological reconstruction of rat ACC LFP electrode placement. Target region was CG1 (AP:+2.7, ML:+0.8, DV:-2.1 from skull surface). Recording electrode placements are indicated with “X”s (n=11).

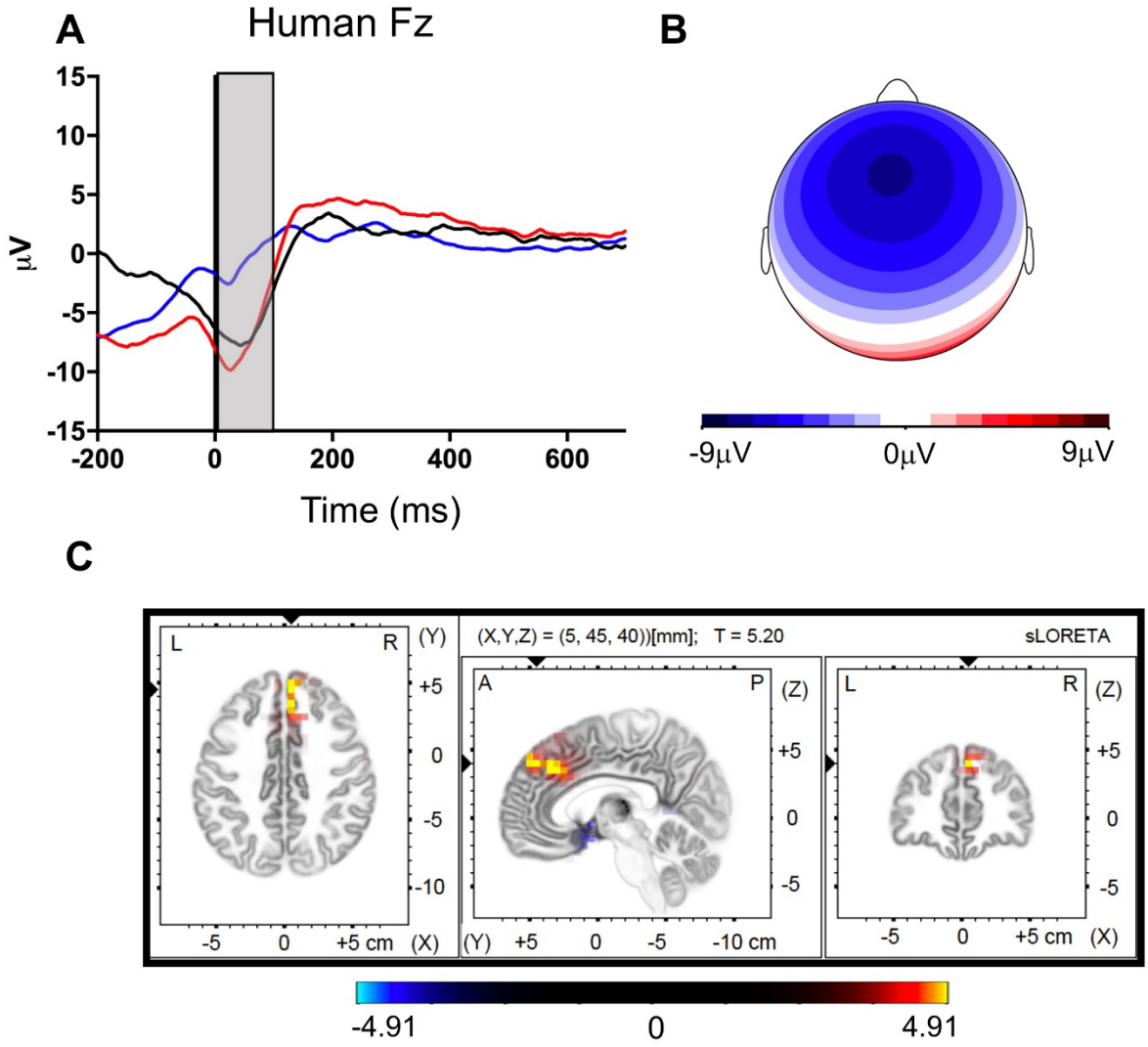

Supplemental Figure 3. Source localization of the human ERN. **(A)** Human FCz (n=26). Errors and correct responses were compared in the 0-100ms time window as indicated by the shaded box. **(B)** Human scalp distribution of the ERN (errors minus correct responses) from 0-100ms post response. **(C)** Source localization of the ERN computed by sLORETA. The peak voxel was located in the medial frontal gyrus (BA6; X=5, Y=45, Z=35; t=5.20, $p<0.05$, corrected), and the cluster surviving correction for multiple comparison encompassed medial prefrontal and anterior cingulate cortices. BA: Broadmann Area. X,Y,Z coordinates are based on Talairach coordinates. A: Anterior, P: Posterior, L: Left, R: Right.

Supplemental Table 2. *sLORETA results for error and congruency effects in humans*

A. *Error minus Correct*	**BA**	**X**	**Y**	**Z**	**t-value**
Medial frontal gyrus	6	5	45	35	5.20
	9	5	31	31	5.14
Middle temporal gyrus	21	-64	-20	-7	4.97
Medial frontal gyrus	9	5	36	30	4.95
	6	5	36	35	4.92
B. *Incongruent minus Congruent*	**BA**	**X**	**Y**	**Z**	**t-value**
Frontal Lobe Precentral Gyrus	6	59	2	32	6.80
	6	59	6	32	6.58
	6	59	-3	32	6.28
	4	64	-8	28	6.23
	6	64	-3	28	6.15
	6	59	2	37	5.80
	6	59	1	28	5.77
	6	59	-3	37	5.70
	4	64	-13	33	5.68
Parietal Lobe Postcentral Gyrus	3	64	-13	28	5.67
Frontal Lobe Inferior Frontal	9	59	6	27	5.59
Parietal Lobe Postcentral Gyrus	1	64	-18	33	5.37
Frontal Lobe Inferior Frontal	9	59	11	27	5.27
Parietal Lobe Postcentral Gyrus	1	64	-18	29	5.23
Frontal Lobe Precentral Gyrus	6	59	-8	37	5.14
	4	59	-13	33	4.98
Frontal Lobe Inferior Frontal	9	54	6	32	4.94
Frontal Lobe Middle Frontal Gyrus	9	54	7	37	4.85
	9	54	12	36	4.79
Parietal Lobe Postcentral Gyrus	2	64	-23	33	4.79
Frontal Lobe Medial Frontal Gyrus	10	-5	59	20	4.79
Frontal Lobe Precentral Gyrus	6	54	2	32	4.78
Parietal Lobe Inferior Parietal	40	64	-23	29	4.77
Frontal Lobe Middle Frontal Gyrus	10	-30	59	6	4.75
Frontal Lobe Precentral Gyrus	4	59	-13	37	4.74
Frontal Lobe Medial Frontal Gyrus	9	-5	54	16	4.73
Frontal Lobe Superior Frontal	8	-35	22	50	4.72

Table 2. sLORETA results for error and congruency effects in humans. BA: Broadmann Area. X,Y,Z coordinate are based on Talairach coordinates. T-values are displayed that exceeded the threshold for two-tailed $p <. 05$ significance thresholds (t values above 4.91 for error contrast and above 4.71 for congruency contrast).